High-sensitivity sensor based on mode number-encoded multi-longitudinal mode fiber laser

Jiejun Zhang (张杰君), Qizhen Sun (孙琪真)*, Jianghai Wo (沃江海), Xiaolei Li (李晓磊), and Deming Liu (刘德明)

[1]*National Engineering Laboratory for Next Generation Internet Access System (HUST), Wuhan 430074, China*

[2]*School of Optical and Electronic Information Technology, Huazhong University of Science and Technology, Wuhan 430074, China*

**Corresponding author: qzsun@mail.hust.edu.cn*

Received July 5, 2012; accepted October 10, 2012; posted online January 21, 2013

We propose a high sensitivity sensor based on a mode number-encoded multi-longitudinal mode fiber laser. The fiber laser incorporates a uniform fiber Bragg grating (FBG) and a fiber Fabry-Perot interferometer (FFPI) as sensitive components in the cavity. The sensor counts the number of longitudinal modes (NLM) of fiber laser, which is caused by the mismatch between the reflection band of FBG and the transmission band of FFPI resulting from the application of external perturbation to the FBG. An electrical spectrum analyzer is adopted to analyze the NLM. The strain sensor is experimentally demonstrated to have sensitivity of as high as 0.02 $\mu\varepsilon$/mode.

OCIS codes: 060.2370, 140.3510, 280.3420.

doi: 10.3788/COL201311.020605.

Fiber Bragg grating (FBG) sensors have many distinct advantages, such as capability for remote sensing and multiplexing, simplicity of fabrication, immunity from electromagnetic interference, and so on. Thus far, strain and temperature have caught the interest of researchers in this field[1]. In these applications, strain and temperature cause the shifting of the central wavelength of FBG; in addition, the sensitivity of the sensors is mainly determined by interrogating methods for the wavelength shift. Optical spectrum analyzer (OSA) is widely used to measure the reflection and transmission spectra of FBG. Strain and temperature variations can be easily detected by tracking the peaks of the spectra displayed on an OSA. Wavelength-swept laser is a popular tool in a high-accuracy fiber-optic sensor system[2,3], and is demonstrated by employing a narrowband wavelength-scanning filter, such as a fiber Fabry-Perot tunable filter, inside a laser cavity. The wavelength-swept laser can achieve higher resolution compared with the OSA, because it has a narrower linewidth.

Meanwhile, fiber lasers have also attracted great interest in sensing applications[4]. The sensor implementation of the laser is relatively straight forward, i.e., changes in external conditions cause changes in the laser cavity, which may be determined by monitoring the change in some specific characteristics of the output laser. These characteristics include output power, wavelength shift[5], and optical pulse repetition rate of mode-locked fiber lasers. Furthermore, various optical effects, including beating between different longitudinal modes and polarization modes of fiber laser, have been exploited to obtain better performance[6].

In this letter, an interrogation approach based on the number of longitudinal modes (NLM) of laser output is proposed. The sensor inherits the intrinsic merits of wavelength sensing. Unlike other applications of multimode fiber lasers, in which mode hopping and spatial hole burning are deemed detrimental[7], the effect is essential for sensing reliability. High sensitivity of up to 0.02 $\mu\varepsilon$ for strain sensing (equivalent to 0.002 K for temperature sensing) is demonstrated, which is higher than most of the reported fiber sensors.

Figure 1 illustrates the experimental setup. The structure of fiber laser is a hybrid of linear cavity and ring cavity. The ring cavity was constructed by connecting port 1 and port 3 of a circulator through a fiber Fabry-Perot interferometer (FFPI) and a polarization controller (PC). The FFPI comprising two identical FBGs with certain spacing was employed to provide a narrow passband (Fig. 1, inset). The PC was used to stabilize the laser output. In the linear part of the cavity, a 1.5-m piece of erbium-doped fiber (EDF) and a uniform FBG were fusion spliced to port 2 of the circulator. The fiber laser was pumped by a 980-nm laser diode through a 980/1 550 nm wavelength division multiplexer (WDM), after which it was exported from the 1 550-nm port of WDM. The output was split by a 3-dB coupler, and then transmitted to an OSA and a high speed photo detector, respectively. The electric signal from the detector was analyzed by an electrical spectrum analyzer (ESA).

The working principle can be described as follows. The variation of measurants causes the wavelength shift of the FBG spectrum as well as the resulting mismatch between

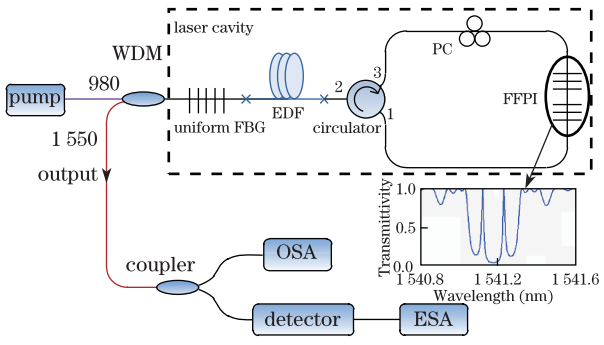

Fig. 1. Schematic illustration of the sensing system.

the reflection band of uniform FBG and the transmission band of FFPI. The wavelength range satisfying the lasing condition also varies, and is interpreted as the variation of NLM.

The round-trip loss of the cavity at wavelength λ is given by

$$\alpha(\lambda) = 1 - (1 - \alpha_{\mathrm{C}}) \cdot R_{\mathrm{FBG}}(\lambda) \cdot T_{\mathrm{FFPI}}(\lambda), \quad (1)$$

where α_{C} denotes the wavelength-independent cavity loss induced by incorporated components and fusion splicing, which is estimated to be 4.6 dB; $R_{\mathrm{FBG}}(\lambda)$ and $T_{\mathrm{FFPI}}(\lambda)$ represent the reflectivity of the uniform FBG and transmittivity of the FFPI at wavelength λ, respectively. The threshold condition of the fiber laser is given as

$$g^2(1 - \alpha(\lambda)) > 1, \quad (2)$$

where g is the small signal gain of EDF under certain pump power, and is considered to be wavelength-independent within the concerned wavelength domain (i.e., narrow passband of FFPI). Typical values for hole-width and hole-depth in spectral hole burning of EDF are broader than 2 nm and less than 1 dB, respectively; thus, the small signal gain is sufficient to give an accurate calculation[8]. Substituting Eqs. (1) to (2), we can derive the threshold condition as

$$R_{\mathrm{FBG}}(\lambda) T_{\mathrm{FFPI}}(\lambda) > 1/\left[g^2(1 - \alpha_{\mathrm{C}})\right]. \quad (3)$$

The wavelength range $\Delta\lambda$ satisfying Eq. (3) can be calculated numerically. It determines the number of available longitudinal modes N in the output laser as follows:

$$N = \mathrm{ceil}(\Delta\lambda/\Delta\lambda_{\mathrm{FSR}}), \quad (4)$$

where ceil rounds the result to the nearest integer towards infinity, and $\Delta\lambda_{\mathrm{FSR}}$ is the free spectral range (FSR) in wavelength domain, as determined by the length of the laser cavity.

In the sensing system, the adopted uniform FBG has a central wavelength of 1 541.158 nm, reflectivity of 98.7%, and 3-dB bandwidth of 0.159 nm. The FFPI, fabricated by 2 identical 4.7-mm-long FBGs with an interval of 5 mm, had two transmission peaks within the reflection band of each FBG, which were set at 1 541.117 and 1 541.238 nm, respectively. The simulated transmission spectrum of FFPI is shown in Fig. 2. The 3-dB bandwidth of the pass band at 1 541.238 nm is calculated to be 13.2 pm, within which the laser is expected to be achieved. The total length of laser cavity is 5 m, corresponding to an FSR of 20 MHz (or $\Delta\lambda_{\mathrm{FSR}}$=0.16 pm). We calculated $g \approx 2.98$ around 1 541.238 nm, while considering a 1.55-m-long EDF (Verrillon EDF-1-125) under a pump power of 80 mW.

Often, measurands, such as temperature or strain, influence $\Delta\lambda$. Figure 2 shows an example of the strain-sensing process. As can be seen, the blue curve is the transmission spectrum of FFPI around the second transmission band. The solid and dotted red curves are the reflection spectra of uniform FBG under strain1 and strain2, respectively. The solid and dotted black lines represent the values corresponding to the left side of Eq. (3) under strain1 and strain2, respectively. The green line is the value corresponding to the right of Eq. (3). Here, $\Delta\lambda$ is considered the wavelength range as the black curve is above the green line. In the simulation, the difference between strain1 and strain2 is 2 $\mu\varepsilon$. Under strain1, $\Delta\lambda_1$=4.5 pm. According to Eq. (4), NLM in the laser output is N_1=29. Similarly, we have $\Delta\lambda_2$=8.7 pm and N_2=55 under strain2. Thus, NLM increases by 26 as a result of 2 $\mu\varepsilon$ change on uniform FBG.

Figure 3 plots the simulation results of the impact of the strain applied to the uniform FBG on $\Delta\lambda$ and the subsequent NLM. Sensitivity is higher than 0.03 $\mu\varepsilon$ per mode when the strain changes from 0 to 0.4 $\mu\varepsilon$; in addition, the average sensitivity within the range is about 0.05 $\mu\varepsilon$. Such sensitivity is two orders of magnitude higher than most of the reported strain sensors ($\sim$1 $\mu\varepsilon$). In fact, it is possible to further improve sensitivity by utilizing a fiber laser with a longer cavity, which has a smaller FSR. In that case, wavelength-selective components (i.e., uniform FBG and FFPI) with steeper edges of reflection or transmission bands are desirable in ensuring sufficient loss difference between two adjacent modes.

In the experiment, the uniform FBG was installed on two motion stages with spacing of 60 cm. The resolution of motion stages was set to 30 nm, resulting in strain change of FBG in steps of 0.05 $\mu\varepsilon$. Beat spectra were measured every two steps (0.1 $\mu\varepsilon$). The number of beat spectrum peaks represents NLM[9]. Figure 4 displays the beat spectrum of output laser under different applied strains. As a result of 0.1 $\mu\varepsilon$ strain change, NLM decreases from 17 to 11 and then to 6 (Figs. 4 (a), (b), and (c)). It can be deduced that strain sensitivity is 0.02 $\mu\varepsilon$ per mode number change in the experiment. Mode hoping, which causes random power distribution among

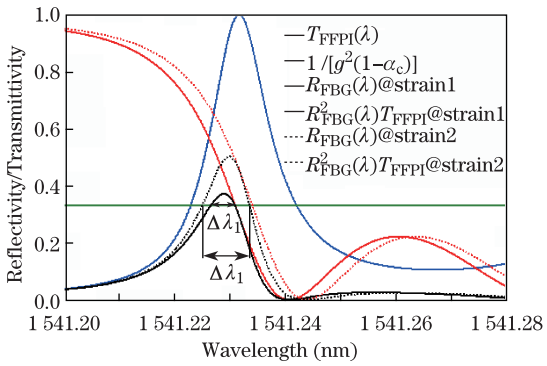

Fig. 2. (Color online) Schematic diagram of a strain sensing process.

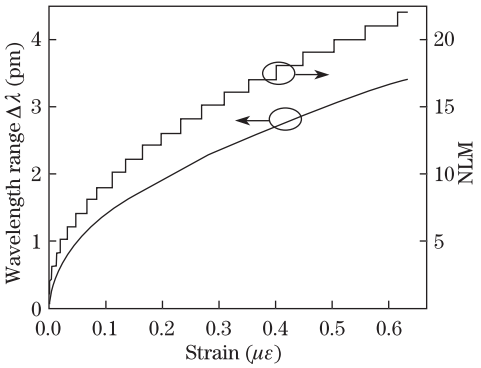

Fig. 3. Wavelength range satisfying the threshold condition and the corresponding mode number as a function of the strain applied to FBG.

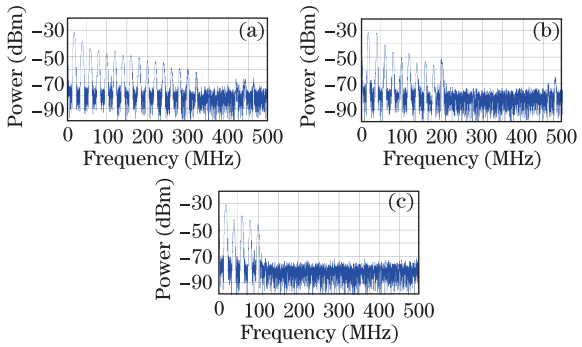

Fig. 4. Measured spectra of beat signal from ESA under resolution bandwidth of 3.0 MHz. The strain applied on the uniform FBG decreases in a step of 0.1 $\mu\varepsilon$ from (a) to (c).

every longitudinal mode, ensures that all modes within $\Delta\lambda$ are excited. Given that EDF is in the linear part of laser cavity, spatial hole burning can prevent any longitudinal mode from being too dominant. These effects are essential in generating the highest order of beat frequency (peaks at 320 Fig. 4(a), 200 Fig. 4(b), and 100 MHz Fig. 4(c)) and in the correct counting of NLM. Although the relative heights of the peaks are unstable because of mode competition, the number of peaks remains constant under certain amounts of strain, ensuring the reliability of the sensor. The slight variation between experiment and theory might be due to the discreteness of NLM, which can be avoided through proper calibration in practical use.

In addition, both sensitivity and measurement range of the sensor can be further improved. First, $\Delta\lambda_{\mathrm{FSR}}$ in Eq. (4) can be made smaller using a longer laser cavity. Thus, more NLM changes are induced for a certain strain variation, indicating higher sensitivity. Second, if we optimally design the FFPI to have a wider transmission band, the possible maximum NLM for the fiber laser increases, thus allowing a larger measurement range.

Given that temperature has a similar influence on FBG, the sensor can also be used as a temperature sensor. By comparing the thermo-coefficient and elasto-coefficient of silica fiber[10,11], the sensitivity is estimated to be 0.002 K per mode change.

Multiple lasers with different cavity lengths are obtained by employing cascaded FBGs with different Bragg wavelengths corresponding to the different transmission bands of the FFPI. Beat frequencies generated by longitudinal modes of different lasing wavelengths are usually larger than 10 GHz, as determined by the wavelength spacing of the multi-wavelength laser; thus it does not cause any interference in counting NLM. The bandwidths of the beat frequencies of certain laser cavities are extremely narrow compared with FSR of the cavity (i.e., mode spacing seen from the beat spectrum Fig. 4) due to the phase-coherency of all the longitudinal modes. This feature provides enough room for many sets of different beat frequencies. As a result, the sensor multiplexing scheme with a large number can be achieved. Assisted by frequency spectrum interrogation with high resolution bandwidth, beat frequencies of longitudinal modes from different sensing FBGs can be precisely measured and analyzed in terms of which laser cavity they belong to. Thus, the information coming from different sensors can be distinguished and demodulated.

In conclusion, a longitudinal-mode-number encoded sensor based on a multi-mode fiber laser is exploited. The value of strain can be obtained by counting the peaks of the beat spectrum of the multi-longitudinal mode laser. A high sensitivity up to 0.02 $\mu\varepsilon$ per mode for a strain sensor is demonstrated in the experiment. The sensor is immune to optical power jitter and electromagnetic interference owing to the fact that the sensing information is mode number-encoded. Simplicity for multiplexing and signal processing is also noteworthy. Sensor multiplexing is obtained through high resolution frequency interrogation and analysis; this is achieved by employing cascaded FBGs with varied Bragg wavelengths corresponding to the different cavity lengths and transmission bands of the FFPI. Given that all beat frequencies are harmonic of FSR, many existing compact devices, which are widely used to monitor the high order harmonic frequency in AC power transition systems[12], can greatly facilitate the signal processing of the sensor. The sensing range and sensitivity of the sensor can be further improved using FFPI with wider transmission band and by increasing the length of laser cavity. The proposed fiber laser sensor can find broad applications in high sensitivity sensing.

This work was supported by the Major Program of National Natural Science Foundation of China (No. 60937002), the National Natural Science Foundation of China (No. 60907037), and the Fundamental Research Funds for the Central Universities (HUST: 2011TS059).

References

1. M. Majumder, T. K. Gangopadhyay, A. K. Chakraborty, K. Dasgupta, and D. Bhattacharya, Sensors Actuators Phys. **147,** 150 (2008).
2. B. C. Lee, E. J. Jung, C. S. Kim, and M. Y. Jeon, Meas. Sci. Technol. **21,** 094008 (2010).
3. E. J. Jung, C. S. Kim, M. Y. Jeong, M. K. Kim, M. Y. Jeon, W. Jung, and Z. Chen, Opt. Express **16,** 16552 (2008).
4. K. Grattan and T. Sun, Sensors Actuators Phys. **82,** 40 (2000).
5. A. C. L. Wong, W. Chung, C. Lu, and H. Y. Tam, IEEE Photon. Technol. Lett. **22,** 1464 (2010).
6. G. Ball, G. Meltz, and W. Morey, Opt. Lett. **18,** 1976 (1993).
7. H. S. Kim, S. K. Kim, and B. Y. Kim, Opt. Lett. **21,** 11441 (1996).
8. S. Fukushima, C. Silva, Y. Muramoto, and A. J. Seeds, J. Lightwave Technol. **21,** 3043 (2003).
9. M. Bolshtyansky, J. Lightwave Technol. **21,** 1032 (2003).
10. Y. J. Rao, Meas. Sci. Technol. **8,** 355 (1997).
11. K. O. Hill and G. Meltz, J. Lightwave Technol. **15,** 1263 (1997).
12. P. E. Sutherland, IEEE Trans. Ind. Appl. **31,** 175 (1995).